

A Biochemical Model of Photosynthetic CO₂ Assimilation in Leaves of C₃ Species

G.D. Farquhar¹, S. von Caemmerer¹, and J.A. Berry²

¹ Department of Environmental Biology, Research School of Biological Sciences, Australian National University, P.O. Box 475, Canberra City ACT 2601, Australia and

² Carnegie Institution of Washington, Department of Plant Biology, Stanford, Cal. 94305, USA

Abstract. Various aspects of the biochemistry of photosynthetic carbon assimilation in C₃ plants are integrated into a form compatible with studies of gas exchange in leaves. These aspects include the kinetic properties of ribulose biphosphate carboxylase-oxygenase; the requirements of the photosynthetic carbon reduction and photorespiratory carbon oxidation cycles for reduced pyridine nucleotides; the dependence of electron transport on photon flux and the presence of a temperature dependent upper limit to electron transport. The measurements of gas exchange with which the model outputs may be compared include those of the temperature and partial pressure of CO₂ ($p(\text{CO}_2)$) dependencies of quantum yield, the variation of compensation point with temperature and partial pressure of O₂ ($p(\text{O}_2)$), the dependence of net CO₂ assimilation rate on $p(\text{CO}_2)$ and irradiance, and the influence of $p(\text{CO}_2)$ and irradiance on the temperature dependence of assimilation rate.

Key words: Electron transport – Leaf model – Light and CO₂ assimilation – Ribulose biphosphate carboxylase-oxygenase – Temperature – Photosynthesis (C₃).

Introduction

The present study aims to integrate current knowledge of the functioning of the biochemical components of photosynthetic carbon assimilation in C₃ plants. It results in a model, a further development of those described by Hall and Björkman (1975), Peisker (1976) and Berry and Farquhar (1978), which suc-

Abbreviations: RuP₂=ribulose biphosphate; PGA=3-phosphoglycerate; C= $p(\text{CO}_2)$ =partial pressure of CO₂; O= $p(\text{O}_2)$ =partial pressure of O₂; PCR=photosynthetic carbon reduction; PCO=photorespiratory carbon oxidation

ceeds in relating studies of enzyme kinetics and whole chain electron transport to those of gas exchange of whole leaves.

We first describe overall processes in the leaf, then analyse the partial processes at the organelle level, and finally attempt to describe the overall system in terms of its component parts.

Model Development

1. Limitations to the Rate of Assimilation of CO₂

1.1. Dark Reactions. The photosynthetic carbon reduction (PCR) and photorespiratory carbon oxidation (PCO) cycles are linked by an enzyme common to both, viz. ribulose biphosphate (RuP₂) carboxylase-oxygenase (Fig. 1). In the PCO cycle, when the enzyme catalyses the reaction of RuP₂ with one mol of O₂, 0.5 mol of CO₂ is released. Thus the net rate of CO₂ assimilation is

$$A = V_c - 0.5 V_o - R_d^1 \quad (1)$$

where V_c is the rate of carboxylation, and V_o the rate of oxygenation. The symbol R_d represents CO₂ evolution from mitochondria in the light, other than that associated with the PCO cycle. Mitochondrial oxygen uptake and electron transport associated with normal dark respiration are likely to be inhibited by illumination but CO₂ release may continue (Graham 1979). For want of a better term we call this “dark respiration”.

Graham (1979) has reviewed the conflicting evidence on the effects of light on “dark respiration”, and concluded himself that dark respiration in the light is a significant part of the carbon lost by the plant. We assume no effect of light on the CO₂ flux, R_d , but recognise that this is an oversimplification.

¹ Symbols and units are listed at the end of this article

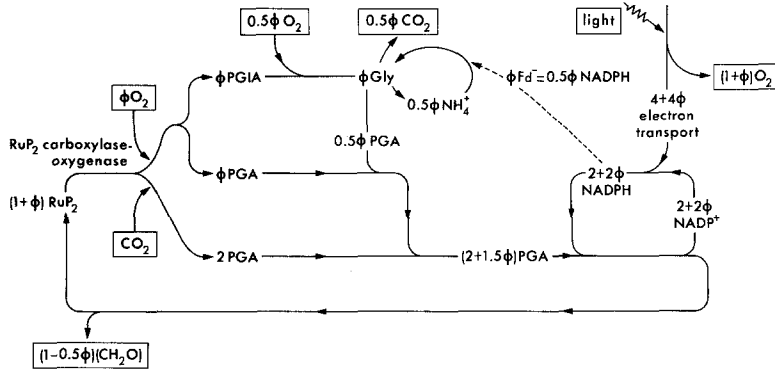


Fig. 1. Simplified photosynthetic carbon reduction (PCR) and photorespiratory carbon oxidation (PCO) cycles, with cycle for regeneration of NADPH linked to light driven electron transport. For each carboxylation, ϕ oxygenations occur. Gly denotes glycine, Fd⁻ denotes reduced ferredoxin (assumed equivalent to 1/2 NADPH), PGA denotes 3-phosphoglycerate, PGIA phosphoglycolate. At the compensation point $\phi = 2$

If the enzyme reaction is ordered with RuP₂ binding first, carboxylation and oxygenation velocities are given by (Farquhar 1979)

$$V_c = V_{c_{\max}} \frac{C}{C + K_c(1 + O/K_o)} \cdot \frac{R}{R + K'_r}$$

$$= V_{c_{\max}} \frac{C/K_c}{1 + C/K_c + O/K_o} \cdot \frac{R/K'_r}{1 + R/K'_r} \quad (2)$$

and

$$V_o = V_{o_{\max}} \frac{O}{O + K_o(1 + C/K_c)} \cdot \frac{R}{R + K'_r}$$

$$= V_{o_{\max}} \frac{O/K_o}{1 + C/K_c + O/K_o} \cdot \frac{R/K'_r}{1 + R/K'_r} \quad (3)$$

where $V_{c_{\max}}$ and $V_{o_{\max}}$ are the maximum velocities of the carboxylase and oxygenase, respectively, C and O are the partial pressures of CO₂ and O₂, $p(\text{CO}_2)$ and $p(\text{O}_2)$ respectively, in equilibrium with their dissolved concentrations in the chloroplast stroma; K_c and K_o are the Michaelis-Menten constants for CO₂ and O₂; R is the concentration of free (unbound) RuP₂ and K'_r is the effective Michaelis-Menten constant for RuP₂.

Dividing (3) by (2) we obtain ϕ , the ratio of oxygenation to carboxylation.

$$\phi = \frac{V_o}{V_c} = \frac{V_{o_{\max}}}{V_{c_{\max}}} \cdot \frac{O/K_o}{C/K_c} \quad (4)$$

For each carboxylation, ϕ oxygenations occur.

We see that several factors may limit the rate of carboxylation in vivo. Firstly the relative partial pressures of CO₂ and O₂ determine the partitioning between carboxylation and oxygenation. Secondly, the amount of activated enzyme present determines the maximum velocity, $V_{c_{\max}}$ (and, therefore $V_{o_{\max}}$). Thirdly, the rate of regeneration of acceptor, RuP₂, determines the concentration of free RuP₂. The re-

generation rate itself is usually limited by the supply of NADPH and ATP.

1.2. NADPH and ATP Requirements. Each carboxylation produces two molecules of 3-phosphoglycerate (PGA); each PGA is first phosphorylated and then reduced, requiring one ATP and one NADPH molecule. Each oxygenation produces one molecule of PGA and one of phosphoglycolate. In turn one mole of phosphoglycolate produces 0.5 mol of PGA. Thus:

$$\text{rate of PGA production} = 2V_c + 1.5V_o \quad (5)$$

The events that follow oxygenation of 1 mol RuP₂ include release and refixation of 0.5 mol ammonia (Woo et al. 1978; Keys et al. 1978), a sequence which requires the use of 2 Fd⁻ (reduced ferredoxin) per NH₄⁺. The PCO cycle therefore appears to have an additional cost of 0.5 NADPH for each 0.5 NH₄⁺ refixed. Thus:

$$\begin{aligned} \text{rate of NADPH consumption} &= \text{rate of PGA production} \\ &+ \text{rate of NH}_4^+ \text{ refixation} \\ &= (2V_c + 1.5V_o) + 0.5V_o \end{aligned}$$

Using (4)

$$= (2 + 2\phi)V_c. \quad (6)$$

It has similarly been shown (Berry and Farquhar 1978), that

$$\text{rate of consumption of ATP} = (3 + 3.5\phi)V_c \quad (7)$$

1.3. Photosynthetic Electron Transport. The rates of production of NADPH and ATP depend on the rate of photosynthetic electron transport. Two electrons are required for the generation of one NADPH. Thus from Eq. (6) an electron transport rate of $(4 + 4\phi)V_c$ is required to meet the rate of NADPH consumption. ATP is produced by photophosphorylation of ADP, and controversy exists over linkage with electron

transport; the number of ATP produced per electron pair (ATP/2e) is variously estimated as 1, 1.33 or 2 and may be flexible (Heber 1976). Using Eq. (7) the rate of electron transport required to sustain the necessary ATP use is $(6+7\phi)V_c \div (\text{ATP}/2e)$.

A limitation to electron transport occurs when insufficient quanta are absorbed. If one quantum must be absorbed by each of the two photosystems to move an electron from the level of H₂O to the level of NADP⁺, the potential rate of electron transport, J , will be related to the absorbed photon flux, I , by

$$J = 0.5(1-f)I \quad (8)$$

where f is the fraction of light lost as absorption by other than the chloroplast lamellae. The fraction f may increase with leaf thickness. There is an upper limit to photosynthetic electron transport which may limit photosynthesis in vivo (Armand et al. 1978). Intrinsic properties of the thylakoid membranes, such as the pool sizes of intersystem intermediates place one limitation, J_{\max} , on the maximum rate of electron transport. J_{\max} is lower in shade leaves than in sun leaves (Björkman et al. 1972). Equation (8) can only hold when $J < J_{\max}$. The incorporation of this upper bound is discussed in an appendix. We later discuss further limitations on electron transport, imposed by insufficient concentrations of ADP and NADP⁺.

Following Berry and Farquhar (1978), we could write that the velocity of carboxylation is either at the RuP₂ saturated rate, W_c , where

$$W_c = V_{c_{\max}} \cdot \frac{C}{C + K_c(1+O/K_o)} \quad (9)$$

or, limited by RuP₂, at the rate, J' .

J' is the maximum rate of carboxylation allowed by the electron transport. It is determined by the potential rate of electron transfer, J , at the particular irradiance and temperature and is derived from Eq. (6) as

$$J' = \frac{J}{2(2+2\phi)}. \quad (10)$$

(The additional 2 in the denominator arises from the requirement of two electrons per NADPH.)

Thus

$$V_c = \min \{W_c, J'\} \quad (11)$$

where $\min \{ \}$ denotes 'minimum of'.

However, the actual rate will be less than $\min \{W_c, J'\}$. Specifically, the availability of ADP and NADP⁺, which is dependent on the dark reactions of carbon assimilation, also influences the rates of ATP

and NADPH production. West and Wiskich (1968) coined the term 'photosynthetic control' for the ADP dependence of electron transport and associated oxygen production.

2. Integrating the Rate-Limiting Processes at the Chloroplast Level

We will now follow Hall and Björkman (1975) and Peisker (1976) and treat the system as three interacting cycles – the PCR and PCO cycles and one for the input of chemical energy by the photosystems. Eq. (11) will emerge as a limiting case of perfect coupling of the photochemical cycle with the other two. In order to do this we first consider the fluxes at the level of the individual organelles. We use lower case letters for fluxes expressed on this basis.

2.1. RuP₂ Carboxylase-Oxygenase. In Appendix 2, it is shown that at the high enzyme concentrations found in vivo, the rate of carboxylation, v_c , is related to the total concentration (free plus bound) of RuP₂, R_t , by

$$v_c = k'_c R_t \quad (12)$$

where

$$k'_c = \frac{k_c C}{C + K_c(1+O/K_o)} \quad (13)$$

k_c is the turnover number of the carboxylase site, which is 1.7 s⁻¹ in purified enzyme from *Atriplex glabriuscula* at 25 C (Badger and Collatz 1977), and 3.4–3.9 at 30 C in freshly prepared crude extracts from spinach chloroplasts (Badger, pers. comm.). The disparity is less when the temperature dependence is taken into account. The present model (see Table 1) assumes 2.5 s⁻¹ at 25 C (equivalent to 2.2 μmol CO₂ mg carboxylase⁻¹ min⁻¹). When $R_t > E_t$, (the total concentration of enzyme sites) then

$$v_c = k'_c E_t$$

Thus

$$v_c = \min \{k'_c R_t, k'_c E_t\} \quad (14)$$

and at saturating partial pressures of CO₂

$$v_{c_{\max}} = \min \{k_c R_t, k_c E_t\}. \quad (15)$$

The concentration, E_t , is here taken as 87 μmol (g chl)⁻¹. Since there are 8 catalytic sites per molecule, and the carboxylase has a molecular weight of 550,000 (Jensen and Bahr 1977), this corresponds to 6 g carboxylase/g Chl. Further, since we use a value

Table 1. Kinetic parameters for the activity of RuP₂ carboxylase-oxygenase. The underlined values are those used in the present model

k_c		K_c		Reference
At 25 C (s ⁻¹)	Activation energy (J mol ⁻¹)	At 25 C (μbar)	Activation energy (J mol ⁻¹)	
13.7 ÷ 8 ^a	<u>58,520</u>	810 750 525	<u>59,356</u>	Badger and Collatz (1977) Laing et al. (1974) Badger and Andrews (1974)
<u>2.5</u>		<u>460</u>		Freshly ruptured spinach chloroplasts (Badger, personal communication)
k_o		K_o		Reference
mbar				
0.18 k_c	<u>58,520</u>	265 640	<u>35,948</u>	Badger and Collatz (1977) Laing et al. (1974)
0.22 k_c		158		Badger and Andrews (1974)
<u>0.21 k_c</u>		<u>330</u>		

^a Division by 8 is necessary since sites rather than molecules form the basis of the present treatment

for k_c of 2.5 s⁻¹ at 25 C this corresponds to a maximum rate, $k_c E_t$, of 218 μmol (g Chl)⁻¹ s⁻¹.

From Appendix 2,

$$\frac{V_{o_{\max}}}{V_{c_{\max}}} = \frac{k_o}{k_c} \quad (16)$$

where k_o , the turnover number for the oxygenase, is 0.21 times that of the carboxylase at 25 C (cf 0.22 at 25 C determined by Badger and Andrews (1974)). Thus Eq. (4) may be rewritten as

$$\phi = \frac{k_o}{k_c} \frac{O/K_o}{C/K_c} \quad (17)$$

Using the values in Table 1, ϕ is 0.27 at 25 C and partial pressures of CO₂ and O₂ of 230 μbar and 210 mbar respectively, values typical of those inside leaves of C₃ plants (Wong 1979). The rate of oxygenation, v_o , is given by

$$v_o = \phi v_c \quad (18)$$

2.2. Pool Sizes. There is evidence (Heldt 1976) that the total concentration of phosphate in the chloroplast is conserved. Assuming that the total pool of phosphate in forms other than PGA or RuP₂ is constant, the sum of [PGA] plus 2R_t (RuP₂ contains two phosphates) is constant, at 2R_p, say.

$$[\text{PGA}] + 2R_t = 2R_p \quad (19)$$

R_p is the potential concentration of RuP₂ which would occur if the carboxylase-oxygenase velocity were zero in the light, i.e. in the absence of CO₂ and O₂. Collatz (1978) found in *Chlamydomonas reinhardtii* that the concentration of RuP₂ at low partial pressures of CO₂ and O₂ was 325 μmol (g Chl)⁻¹. In spinach protoplasts he measured a concentration of 100 μmol (g Chl)⁻¹. In the present model a potential concentration, R_p, of 300 μmol (g Chl)⁻¹ is assumed.

The total concentration of pyridine nucleotides in the chloroplast is assumed constant, at N_t, although it emerges that N_t does not appear, even implicitly, in the general solution (Eq. (33)). Thus

$$[\text{NADPH}] + [\text{NADP}^+] = N_t \quad (20)$$

2.3. Electron Transport and the Production and Consumption of NADPH. The potential rate of electron transport, j , (expressed on a chlorophyll basis as μEq (g Chl)⁻¹ s⁻¹), depends only on temperature and quantum flux. The chosen upper limit, j_{\max} , placed on electron transport of 467 μEq (g Chl)⁻¹ s⁻¹ (=1,680 μEq (mg Chl)⁻¹ h⁻¹) at 25 C, derives from the measurements of Nolan and Smillie (1976) on chloroplasts of *Hordeum vulgare* (see Fig. 2).

Two electrons plus two protons are required to convert NADP⁺ to NADPH + H⁺. The potential rate of NADPH production is thus $j/2$. In practice, electron flow and NADPH production will be somewhat limited by the supply of ADP and NADP⁺. The present model assumes first order dependence on

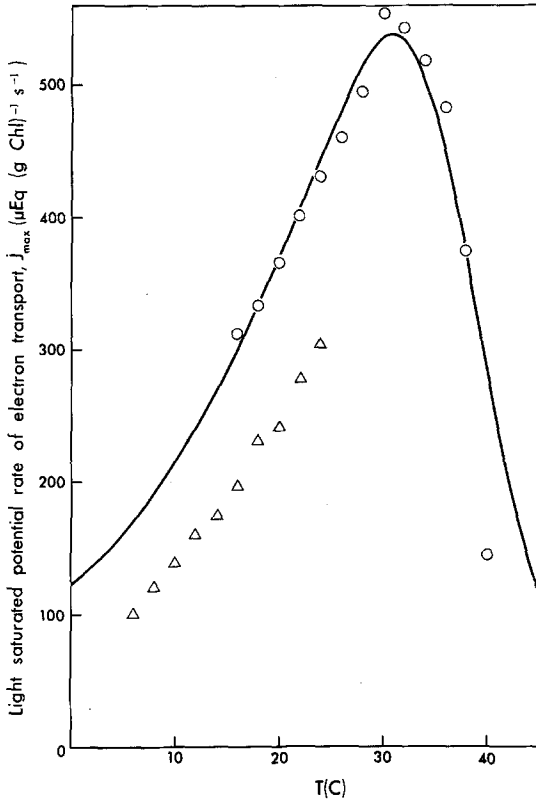


Fig. 2. Temperature dependence of the light saturated potential rate of electron transport, j_{max} . The data are the rates of DCIP reduction (here doubled to obtain rates of electron transport) obtained by Nolan and Smillie (1976) in two batches of chloroplasts from *Hordeum vulgare*. The smooth curve is given by Eq. (36)

$[NADP^+]$, which will be approximately true if the working concentration of $NADP^+$ is similar to the Michaelis constant for its reduction. Thus:

$$\begin{aligned} \text{rate of production of NADPH} &= 1/2 (\text{actual rate of electron transport}) \\ &= 1/2 j \cdot \frac{[NADP^+]}{N_t} \end{aligned} \quad (21)$$

As before,

$$\text{rate of consumption of NADPH} = (2 + 2\phi) v_c \quad (22)$$

Equating the rates of consumption and production (Eqs. (21) and (22))

$$(2 + 2\phi) v_c = \frac{[NADP^+]}{N_t} \cdot \frac{j}{2}$$

and using (20)

$$= \frac{N_t - [NADPH]}{N_t} \cdot \frac{j}{2}$$

Rearranging

$$\frac{[NADPH]}{N_t} = 1 - (4 + 4\phi) v_c / j \quad (23)$$

An equivalent argument may be made for ATP:

$$\frac{[ATP]}{[ATP] + [ADP]} = 1 - \frac{(6 + 7\phi) v_c}{(ATP/2e)j}$$

2.4. Production and Consumption of PGA. As before,

$$\text{rate of production of PGA} = (2 + 1.5\phi) v_c \quad (24)$$

Following Hall and Björkman (1975) and Peisker (1976) we now assume a simplified model of the Calvin cycle in which PGA is "reduced" to RuP_2 , and that the reduction of PGA is first order in $[PGA]$ and in $[NADPH]$. The maximum rate of reduction, m , occurs when $[PGA]$ and $[NADPH]$ equal $2R_p$ and N_t , respectively. Thus

$$\text{rate of reduction of PGA} = \frac{[PGA]}{2R_p} \cdot \frac{[NADPH]}{N_t} \cdot m \quad (25)$$

The parameter, m , a fictional composite from many reactions, determines the degree of coupling between the photochemical cycle on the one hand, and PCR and PCO cycles on the other. In the present outputs, m is made equal to $2k_c E_t$ ($= 436 \mu\text{mol PGA reduced (g Chl)}^{-1} \text{s}^{-1}$ at 25°C). This is sufficiently large to ensure a reasonable coupling and only minimal limitation to photosynthetic rate. Once m is large, its value becomes unimportant, as is true with analogous parameters in the models of Hall and Björkman (1975) and Peisker (1976).

Equating the rate of production of PGA with its rate of reduction (Eqs. (24) and (25))

$$(2 + 1.5\phi) v_c = \frac{[PGA]}{2R_p} \cdot \frac{[NADPH]}{N_t} \cdot m$$

and using (19)

$$= \left(1 - \frac{R_t}{R_p}\right) \cdot \frac{[NADPH]}{N_t} \cdot m \quad (26)$$

2.5. Calculation of RuP_2 Concentration. The concentration of total (free plus bound) RuP_2 , R_t , is found by substituting Eq. (23) in (26) and rearranging

$$\frac{R_t}{R_p} = 1 - \frac{(2 + 1.5\phi) v_c}{1 - (4 + 4\phi) v_c / j} \cdot \frac{1}{m}$$

i.e.

$$\frac{R_t}{R_p} = 1 - \frac{v_c}{1 - v_c / j'} \cdot \frac{1}{m'} \quad (27)$$

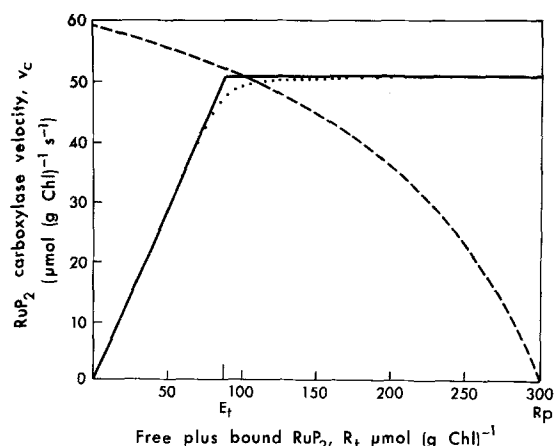


Fig. 3. RuP₂ carboxylase velocity, v_c , versus concentration, R_t , of free plus bound RuP₂. The solid line represents the straight line approximations (Eqn. 14) to the hyperbolic equation (A3) (the dotted line) discussed in Appendix 2. The dashed line represents the dependence of RuP₂ pool size, R_t , on velocity as described by Eq. (27), but plotted 'backwards' as the independent vs dependent variable. The intersection of the solid and dashed lines, the solution of the model, is given by Eq. (33). Standard conditions are $C = 230 \mu\text{bar}$, $O = 210 \text{mbar}$, $T = 25 \text{C}$, $I = 1.000 \mu\text{mol photons m}^{-2} \text{s}^{-1}$. E_t is the total concentration of enzyme sites and R_p is the potential concentration of RuP₂ which would occur if v_c were zero

where

$$j' = j / (4 + 4\phi) \quad (28)$$

(cf Eq. (10)) and

$$m' = m / (2 + 1.5\phi). \quad (29)$$

Thus j' is the maximum rate of carboxylation, given the prevailing partial pressures of CO₂ and O₂, allowed by the light reactions and m' is the maximum rate allowed by the PGA reduction reaction (given that ϕ oxygenations occur per carboxylation.)

2.6. Solution of Model at Chloroplast Level. Eq. (14) describes the dependence of carboxylation rate on total (free plus bound) RuP₂ concentration and Eq. (27), dealing with acceptor regeneration, describes the dependence of RuP₂ concentration on enzyme velocity. The simultaneous solution of these equations, illustrated in Fig. 3, gives the actual velocity and RuP₂ concentration that occur. The response of carboxylase rate, v_c , to changes in total RuP₂ concentration, R_t , (the full and dotted lines) is the relationship between v_c and R_t which occurs with changing irradiance. The dotted line is the exact solution (described in Appendix 2) and the full line is the approximation used here. The physiological interpretation of the solution of Eq. (27) (the dashed line) [here plotted inversely as the independent vari-

able, v_c , versus the dependent variable, R_t] is more difficult. It is the effect on [RuP₂] of changes in carboxylase rate, at constant $p(\text{CO}_2)$, $p(\text{O}_2)$ and temperature i.e. at constant ϕ . The response of R_t to changes in v_c caused by changes in $p(\text{CO}_2)$ has a quite different shape.

From Eq. (14) either $v_c = k'_c E_t$ (the RuP₂ saturated rate) or $v_c = k'_c R_t$ (the initial linear response). The latter may be used to substitute for R_t in Eq. (27) yielding for $R_t < E_t$

$$v_c^2 - (j' + p + j' p/m') v_c + j' p = 0 \quad (30)$$

where p is the rate of carboxylation that would occur if the potential pool size, R_p , of acceptors ($= R_t + 1/2 [\text{PGA}]$) were the only limiting factor (and, again, given that ϕ oxygenations occur per carboxylation). Thus:

$$p = k'_c R_p \quad (31)$$

Eq. (30) is solved as

$$v_{c_{R_t < E_t}} = 1/2 \{ j' + p + j' p/m' - [(j' + p + j' p/m')^2 - 4j' p]^{0.5} \}. \quad (32)$$

The general solution is thus

$$v_c = \min \{ k'_c E_t, v_{c_{R_t < E_t}} \}. \quad (33)$$

2.7. Limiting Case of Perfect Coupling. Eq. (30) is analogous to Eqs. (A2) and (A3) in the appendices. In the limit, as m and $m' \rightarrow \infty$, $[\text{PGA}] \rightarrow 0$ in Eq. (25), and Eq. (30) becomes for $R_t < E_t$

$$(v_c - j')(v_c - p) = 0$$

and Eq. (33) becomes

$$v_c = \min \{ k'_c E_t, j', k'_c R_p \}.$$

However, since the total concentration of sites, E_t , is likely to be less than R_p , the potential concentration of acceptors, the solution becomes

$$v_c = \min \{ k'_c E_t, j' \}. \quad (34)$$

This is the case of perfect coupling of the interacting cycles (cf Eq. (11)). The coupling decreases as m decreases.

2.8. Temperature Dependencies. The temperature dependencies of the kinetic properties of RuP₂ carboxylase-oxygenase used in this model are those determined by Badger and Collatz (1977). The Arrhenius functions were normalised with respect to 25C

$$\text{Parameter} = \text{Parameter (25C)} \exp[(T - 298) E / 298 RT] \quad (35)$$

where E is the relevant activation energy² and R is the universal gas constant, and $T(K)$ is the absolute leaf temperature.

The ratio of the solubilities of O₂ and CO₂ increase with temperature and Ku and Edwards (1977) have suggested that photorespiration increases more rapidly with temperature than does carboxylation for this reason. If the fugacities of the substances are the relevant thermodynamic measures (Badger and Collatz 1977) then to the extent that O₂ and CO₂ act as perfect gases the fugacities are identical with the partial pressures and not affected by their solubilities. In the present model photorespiration increases more rapidly than carboxylation because K_o has a lower activation energy than K_c (Laing et al. 1974; Peisker and Apel 1977).

The light saturated potential rate of electron transport (j_{\max}) depends on temperature (Armand et al. 1978). The data of Nolan and Smillie (1976) (Fig. 2) were used to determine the coefficient 483 and parameters E , S and H for use in the following expression

$$j_{\max} = 483 \exp[-E/RT]/(1 + \exp[(ST-H)/RT])$$

$$(= 467 \mu\text{Eq g Chl}^{-1} \text{s}^{-1} \text{ at } 25\text{C}). \quad (36)$$

$T(K)$ is again the absolute temperature of the leaf. Eq. (36) is a simplified version of an equation developed by Sharpe and DeMichelle (1977) to describe the effect of temperature on enzyme inactivation.

The temperature optimum, $T_{\text{opt}}(K)$, of j_{\max} is known to acclimate in different environments (Armand et al. 1978) and the following expression was derived by differentiation of Eq. (36) with respect to T .

$$T_{\text{opt}} = H/(S + R \ln(H/E - 1)).$$

3. Extension from the Chloroplast to the Leaf

To obtain the net rates of photosynthesis of the leaf it is now necessary to sum the contributions from each chloroplast. The gradients of temperature and partial pressure of oxygen within the C₃ leaf are likely to be unimportant. Small gradients of CO₂ partial pressure may develop, but the distribution of light within the leaf is the greatest cause of uncertainty. It would be convenient for the modeller if the leaf were a uniformly absorbing material or if, as some authors have suggested, sufficient reflection occurred within the leaf to ensure that the gradient of light intensity is unimportant. Wong (1979) has observed that leaves of *Eucalyptus pauciflora* have a greater rate of assimilation when illuminated simultaneously on both sides by 1 mmol photons m⁻² s⁻¹ than when illuminated from one side only by 2 mmol photons m⁻² s⁻¹. Nevertheless, many leaves are thinner than those of *E. pauciflora* and we assume uniform intensity through the leaf, recognising that this extension of the model will not be valid in thick leaves.

Extrapolation of v_c from Eq. (33) to V_c , the rate of carboxylation of the whole leaf, is thus simply made by multiplying by the superficial density of chlorophyll, ρ (g Chl m⁻²), here taken as 0.45. Equation (1) becomes

$$A = \rho(1 - 0.5\phi)v_c - R_d.$$

A "dark respiration" rate, R_d , of 1.1 $\mu\text{mol m}^{-2} \text{s}^{-1}$ at 25 C is assumed, equivalent to 1.1% $V_{c\max}$ or 5.8% of A at 230 $\mu\text{bar } p(\text{CO}_2)$, 210 mbar $p(\text{O}_2)$ and 1,000 $\mu\text{mol photons m}^{-2} \text{s}^{-1}$. R_d is assumed to have an activation energy of 66,405 J mol⁻¹.

At the leaf level v_c is replaced by V_c , j' by J' etc. The enzyme limited rate $k'_c E_t$ becomes $V_{c\max}$

$\frac{C}{C + K_c(1 + O/K_o)}$ where $V_{c\max}$ ($\mu\text{mol m}^{-2} \text{s}^{-1}$) equals $\rho k'_c E_t$ (98 at 25C). The maximum rate of electron transport, now J_{\max} ($= \rho j_{\max} = 210 \mu\text{Eq m}^{-2} \text{s}^{-1}$ at 25C), with a loss fraction, f , of 0.23 (discussed in the next section on quantum yield) would correspond to light saturation at 545 $\mu\text{mol photons m}^{-2} \text{s}^{-1}$, but characteristics described in appendix 1 delay this saturation.

4. Predictions of the Model

4.1. Quantum Yield. The quantum yield is defined as the initial slope of the relationship between assimilation rate, A , and irradiance, I .

In the present model, running on the basis of NADPH requirements

$$\lim_{I \rightarrow 0} \frac{\partial A}{\partial I} = \frac{1 - 0.5\phi}{8 + 8\phi} (1 - f). \quad (37)$$

On the basis of ATP requirements

$$\lim_{I \rightarrow 0} \frac{\partial A}{\partial I} = \frac{1 - 0.5\phi}{12 + 14\phi} (\text{ATP}/2e)(1 - f).$$

The apparent quantum yield is often determined as the slope of A vs. I between 50 and 150 $\mu\text{mol photons m}^{-2} \text{s}^{-1}$ and Ehleringer and Björkman (1977) found a value of 0.081 mol CO₂ per mol quanta absorbed at $p(\text{CO}_2)$ greater than 300 μbar , 20 mbar $p(\text{O}_2)$ and 30C. On the other hand, from a series of measurements at atmospheric $p(\text{CO}_2)$ of 325 μbar , 20 mbar $p(\text{O}_2)$ and 30C they obtained the average yield of 0.073. We

² The various activation energies and their equivalent Q_{10} 's are under E in the list of symbols, units and normal values

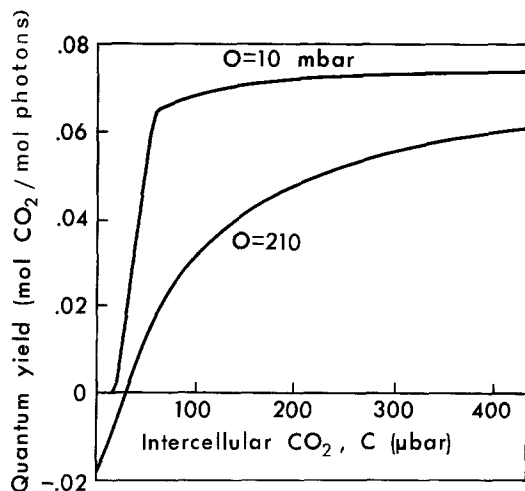


Fig. 4. Quantum yield versus intercellular $p(\text{CO}_2)$, C . The quantum yield is determined as the slope of the curve relating CO_2 assimilation rate, A , to absorbed irradiance, I , in the range $50\text{--}150\ \mu\text{mol photons m}^{-2}\text{ s}^{-1}$ at 25°C . The responses are plotted for two intercellular partial pressures of O_2 , 10 and 210 nbar

chose a value of 0.23 for the loss factor, f ; this empiricism ensures that the model, running on the basis of NADPH requirements has the value 0.077 (the mean of 0.081 and 0.073) at $p(\text{CO}_2)=300$, $p(\text{O}_2)=20$ and 30C . In reality NADPH is also required for other purposes, such as nitrate reduction. If these requirements were taken into account, the fitted parameter, f , would be smaller. The upper bound to quantum yield ($f=0$), set by the requirement of $2\text{ NADPH} + 2\text{H}^+$ (8 quanta) per CO_2 reduced in the absence of oxygenation ($\phi=0$), is 0.125 or, by requirement of 3 ATP per CO_2 reduced is $(\text{ATP}/2e) \div 12$. Assuming a ratio of 1.33 for $(\text{ATP}/2e)$ the latter upper bound is 0.111 and so to obtain the value of 0.077 at 30C in the range 50 to $150\ \mu\text{mol photons m}^{-2}\text{ s}^{-1}$, based on ATP requirements, we would then need to substitute $f=0.13$.

In Fig. 4 the apparent quantum yield is plotted versus partial pressure of CO_2 at 10 mbar and 210 mbar partial pressure of O_2 . At ordinary atmospheric oxygen levels there is a marked increase in quantum yield with increase in $p(\text{CO}_2)$, reflecting diversion of the enzyme from oxygenation to carboxylation, but in 10 mbar $p(\text{O}_2)$ the increase occurs only when $p(\text{CO}_2)$ is less than $60\ \mu\text{bar}$.

Commonly, in C₃ plants the intercellular $p(\text{CO}_2)$ is $230\ \mu\text{bar}$ and $p(\text{O}_2)$ is 210 mbar. At 25°C this means that the ratio, ϕ , of oxygenation to carboxylation is 0.27 (from Eq. (4)) and the initial slope of the A vs. I relationship is, from Eq. (37), $0.066\ \text{mol mol photons}^{-1}$. Over the range $50\text{--}150\ \mu\text{mol photons m}^{-2}\text{ s}^{-1}$ at $230\ \mu\text{bar } p(\text{CO}_2)$ and $210\ \text{mbar } p(\text{O}_2)$ the modelled quantum yield turns out to average 0.051

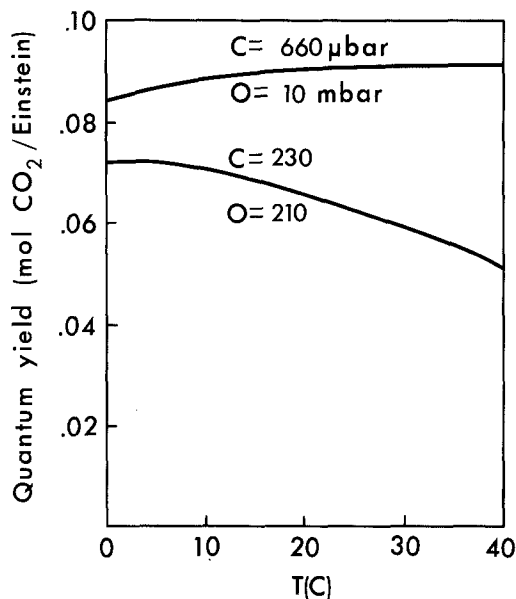


Fig. 5. Quantum yield versus temperature, $T(\text{C})$. The range $0\text{--}10\ \mu\text{mol photons m}^{-2}\text{ s}^{-1}$ has here been used for the determination of the quantum yield. Conditions where photorespiration is minimised (intercellular $p(\text{CO}_2)=600\ \mu\text{bar}$, $p(\text{O}_2)=10\ \text{mbar}$) are contrasted with ambient conditions (intercellular $p(\text{CO}_2)=230\ \mu\text{bar}$, $p(\text{O}_2)=210\ \text{mbar}$)

(see Fig. 4) since under these conditions there is a small degree of curvature in A vs. I . At low and high temperatures, the potential electron transport rate declines (Fig. 2) and the slope of A vs. I diminishes more rapidly with irradiance. For this reason the effects of temperature on quantum yield are plotted in Fig. 5 using the range $0\text{--}10\ \mu\text{mol photons m}^{-2}\text{ s}^{-1}$. At the normal $p(\text{CO}_2)$ and $p(\text{O}_2)$ quantum yield declines with temperature, because the temperature dependence of K_o is greater than that of K_c . At higher $p(\text{CO}_2)$ and lower $p(\text{O}_2)$ the quantum yield is largely independent of temperature.

4.2. Carbon Dioxide Compensation Point. The compensation point, Γ , is defined as that $p(\text{CO}_2)$ at which no net assimilation occurs. In the absence of "dark respiration", the kinetics of the carboxylase-oxygenase are such that Γ increases linearly with $p(\text{O}_2)$, as discussed by Laing et al. (1974) and Peisker (1974). In our notation $\phi=2$ at the compensation point. Thus Γ_* , the compensation point in the absence of "dark respiration", is given by

$$\Gamma_* = \frac{K_c O k_o}{2 K_o k_c} \quad (38)$$

In the presence of "dark respiration", R_d , Γ is given by

$$\Gamma = \frac{\Gamma_* + K_c(1 + O/K_o)R_d/V_{c_{\max}}}{1 - R_d/V_{c_{\max}}} \quad (39)$$

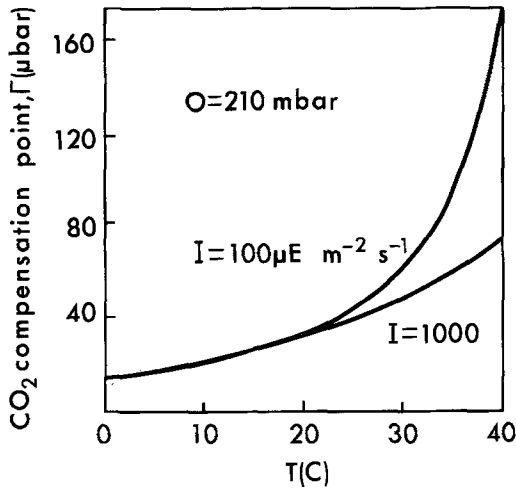


Fig. 6. CO₂ compensation point, Γ (μbar) versus temperature, at two absorbed irradiances (100 and 1,000 $\mu\text{mol photons m}^{-2} \text{s}^{-1}$) and an intercellular $p(\text{O}_2)$ of 210 mbar

and still shows a linear dependence on $p(\text{O}_2)$. At low irradiance, the carboxylase becomes RuP₂ limited ($R_t < E_t$) and $V_{c_{\max}}$ is replaced by $\rho k R_t$ in Eq. (39). The increase of Γ with temperature (Fig. 6) is predicted to be greater at lower irradiances, because "dark respiration" then forms a greater proportion of the CO₂ fluxes. This suggests possible experiments for determining the extent to which "dark respiration" depends on irradiance.

4.3. CO₂ Dependence of Assimilation Rate. In Fig. 7, the rate of carboxylation, V_c , the rate of assimilation, A , and the rate of photorespiratory release of CO₂ (which equals half the rate of RuP₂ oxygenation) are plotted against intercellular $p(\text{CO}_2)$, at the ordinary $p(\text{O}_2)$ of 210 mbar. Carboxylation and assimilation rates increase almost linearly while photorespiration decreases somewhat with increase in $p(\text{CO}_2)$. Curvature commences at $p(\text{CO}_2)$ near that normally found in C₃ plants and corresponds to the point at which the system becomes limited by the regeneration of RuP₂. This is not caused by insufficient irradiance, but by insufficient electron transport capacity, j_{\max} , as found by Lilley and Walker (1975) in isolated spinach chloroplasts. The $p(\text{CO}_2)$ at which this occurs is well below K_c , the Michaelis constant for CO₂. This means that estimation (as, for example, by Tenhunen et al. 1979) of K_c from data on CO₂ assimilation rates in chloroplasts and in whole leaves, even at high irradiance, is liable (Lilley and Walker 1975) to be erroneous. The sharpness of the transition in Fig. 7 is due to our approximation of the dependence of velocity, v_c , on total RuP₂, R_t , by a straight line which abruptly saturates (Eq. (14)), rather than a smoother quadratic (Eq. (A3) in appendix 2) as illustrated in Fig. 3.

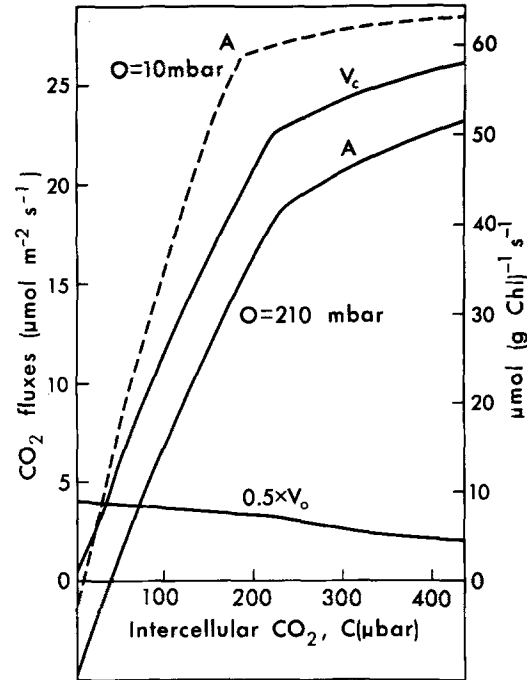


Fig. 7. CO₂ fluxes versus intercellular $p(\text{CO}_2)$, C (μbar). The solid lines at 25°C and 1000 $\mu\text{mol photons m}^{-2} \text{s}^{-1}$ represent the situation in ambient (210 mbar) $p(\text{O}_2)$, with V_c , A and $0.5 \cdot V_o$ denoting the rates of carboxylation, the net rate of assimilation of CO₂ and the rate of release of photorespired CO₂. The dashed line represents the rate of CO₂ assimilation in 10 mbar $p(\text{O}_2)$

The difference between the assimilation rates at 210 mbar and 10 mbar $p(\text{O}_2)$ is sometimes incorrectly used as an estimate of photorespiration. In Fig. 7, the dashed line represents A at 10 mbar $p(\text{O}_2)$ and it is apparent that it greatly exceeds the rate of carboxylation, V_c , sometimes called the 'true photosynthetic rate', at 210 mbar $p(\text{O}_2)$.

In the presence of saturating RuP₂ ($R_t > E_t$), the rate of assimilation is given (from Eqs. (1), (4), (9) and (38)) by

$$A = V_{c_{\max}} \cdot \frac{C - \Gamma_*}{C + K_c(1 + O/K_o)} - R_d \quad (40)$$

The dependence of A on the intercellular $p(\text{CO}_2)$ is then

$$\frac{dA}{dC} = V_{c_{\max}} \cdot \frac{\Gamma_* + K_c(1 + O/K_o)}{[C + K_c(1 + O/K_o)]^2} \quad (41)$$

The initial slope of the A vs. C curve, sometimes called the 'mesophyll conductance', is linearly related to maximal carboxylation velocity and independent of any dark respiration. It is algebraically convenient to evaluate Eq. (41) at $C = \Gamma_*$

$$\frac{dA}{dC} = \frac{V_{c_{\max}}}{\Gamma_* + K_c(1 + O/K_o)} \quad (42)$$

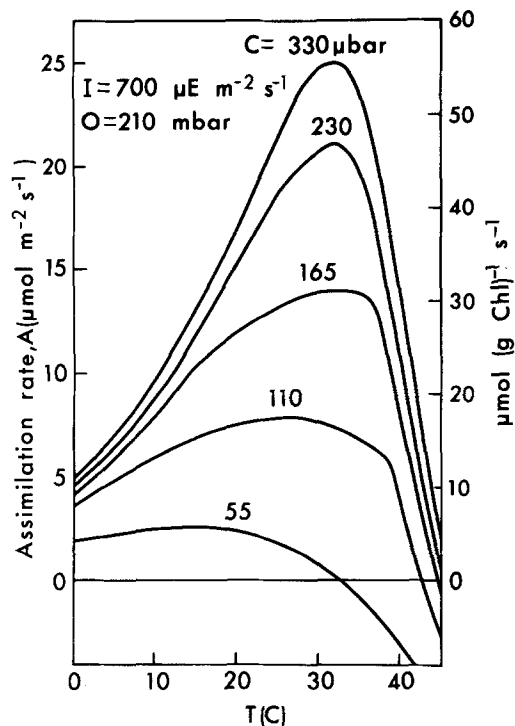


Fig. 8. Effect of intercellular $p(\text{CO}_2)$, C (μbar), on the temperature response of net CO_2 assimilation rate. The absorbed irradiance is $700 \mu\text{mol photons m}^{-2} \text{s}^{-1}$ and the $p(\text{O}_2)$ is 210 mbar

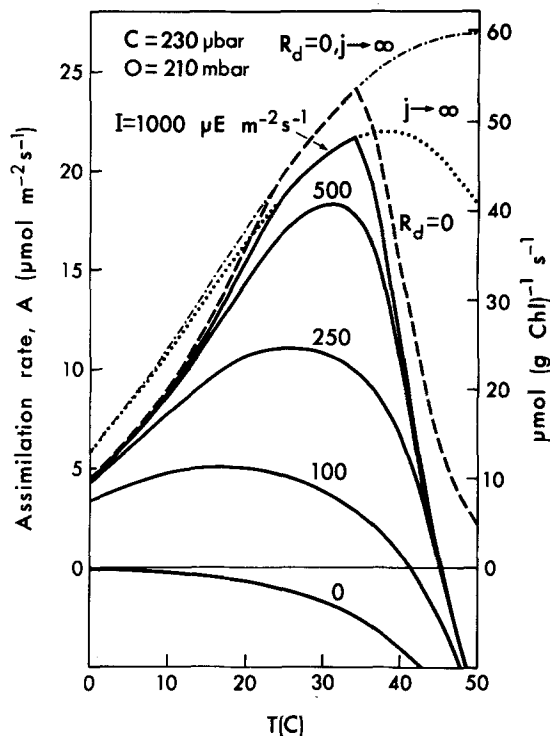


Fig. 9. Effect of absorbed irradiance, I , on the temperature dependence of net CO_2 assimilation rate. The effect of removal of "dark respiration," R_d , is shown as the dashed line and the effect of removal of electron transport limitations (potential electron transport, $j \rightarrow \infty$) is shown as the dotted line. The simultaneous removal of both $R_d=0, j \rightarrow \infty$ is shown as ($\cdot - \cdot -$)

4.4. Temperature Dependence of Assimilation Rate. The temperature optimum for assimilation rate depends inter alia on $p(\text{CO}_2)$ and irradiance. At saturating irradiance this optimum increases with $p(\text{CO}_2)$ over the physiological range (Fig. 8). At low $p(\text{CO}_2)$ the oxygenase function dominates and the photorespiratory release of CO_2 increases with temperature faster than does carboxylation. At higher $p(\text{CO}_2)$, carboxylation dominates and increases with temperature until limited by the maximum rate of electron transport, j_{max} . At a $p(\text{CO}_2)$ of $230 \mu\text{bar}$ the present model has a temperature optimum of 32°C .

At the same intercellular $p(\text{CO}_2)$ of $230 \mu\text{bar}$ the temperature optimum also increases with irradiance (Fig. 9). At low irradiances the temperature response reflects the quantum yield dependence on temperature - the changing pattern of carboxylation and oxygenation as shown in Fig. 5. At high irradiances the temperature response again approaches that of the maximum rate of electron transport, j_{max} , shown in Fig. 2. We must be cautious at temperatures greater than 30°C as the accompanying decreases in j_{max} in Fig. 2 represent damage as much as reversible inactivation. Under the conditions shown in Fig. 9, increasing "dark respiration", R_d , shown as the nega-

tive assimilation rate at $0 \mu\text{mol photons m}^{-2} \text{s}^{-1}$, does not significantly affect the temperature optimum; the effect of its removal is shown as the dashed line. Removal of the limitation on electron transport ($j \rightarrow \infty$, shown by the dotted line) increases the optimum to 38°C . When "dark respiration" and electron transport limitation are both removed (shown as $\cdot - \cdot -$ in Fig. 9) the optimum shifts to 50°C . The latter optimum largely reflects the temperature effects on the Michaelis constants for CO_2 and O_2 . However, the data on which these are based (Badger and Collatz 1977) were obtained in the range 5 – 35°C , and we must again be cautious in extrapolating. In the present model, as in vivo, the temperature optimum depends on the interplay of a number of processes.

4.5. Effects of Leaf Nitrogen Content. In all the previous figures E_t has been kept at $87 \mu\text{mol site (g Chl)}^{-1}$ equivalent to $6 \text{ g carboxylase/g Chl}$ or, with a chlorophyll density of 0.45 g m^{-2} , to a V_{cmax} of $98 \mu\text{mol m}^{-2} \text{s}^{-1}$. The effects of reducing the enzyme: chlorophyll ratio to 3 g/g and 1 g/g are shown in Fig. 10 (the "dark respiration" rates were scaled down proportionally). The plots represent the re-

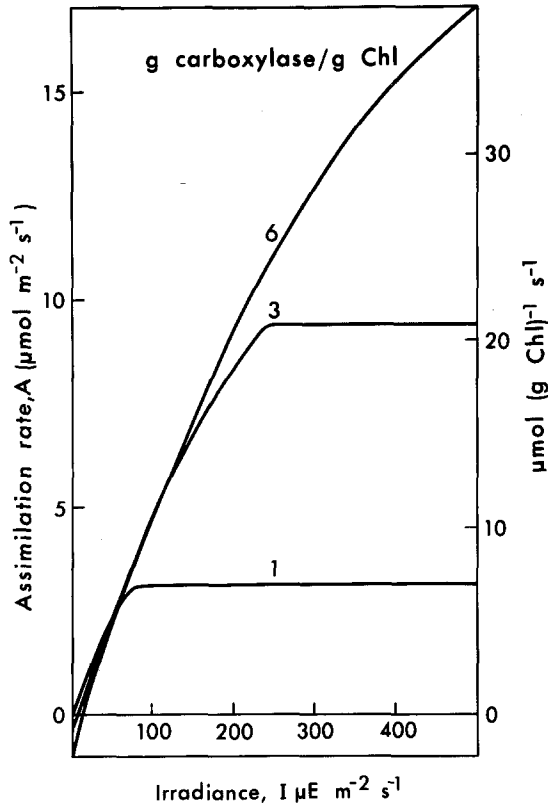


Fig. 10. Rate of assimilation of CO₂, A , versus absorbed irradiance, I , at three levels of carboxylase - 6, 3 and 1 g carboxylase/g chlorophyll. Rates of "dark respiration" are scaled accordingly

sponses of assimilation rate, A , to irradiance, I . The hypothetical leaf at lower carboxylase levels has initially higher assimilation rates but is unable to take advantage of higher irradiances. The responses appear similar to those observed by Björkman et al. (1972) in leaves of *Atriplex patula* grown at different irradiances.

Photosynthesis at the leaf level may be described without reference to chlorophyll. Thus, at 25°C, $V_{c_{max}}$ ($\mu\text{mol m}^{-2} \text{s}^{-1}$) is given by $\frac{10^6 \cdot 8 \cdot 2.5}{550000}$ (=36) times the superficial density (g m^{-2}) of RuP₂ carboxylase (from properties described in Sect. 2.1). Since 6.25 g protein usually contain 1 g nitrogen, $V_{c_{max}}$ is 227 times the density (g m^{-2}) of N in the carboxylase. In the present model, $A = 0.19 V_{c_{max}}$ (at our standard conditions) i.e. 43 times the density (g m^{-2}) of N as RuP₂ carboxylase. If the ratio of carboxylase nitrogen to total nitrogen in a leaf is x , then the present model predicts that the assimilation rate ($\mu\text{mol m}^{-2} \text{s}^{-1}$) of the leaf at 25°C and saturating irradiance should be approximately $43x$ times its nitrogen density (g m^{-2}); at 30°C the factor becomes $51x$. In experiments in which the nitrogen nutrition of *Gossypium hirsutum* was varied, Wong (1979) found that the assimilation

rate at 30°C was roughly 20 times the nitrogen density. We believe that the increased superficial density of carboxylase and associated electron transport capacity in thicker leaves is likely to be the primary cause of observed increased rates of assimilation (Singh et al. 1974; Charles-Edwards, in press). The increased surface area of the mesophyll cells, emphasised by Nobel et al. (1975), is likely to be an associated requirement which allows expression of these other primary changes.

Conclusion

We have integrated process at the sub-organelle level using, as far as possible, data obtained at this same organisational level. Nevertheless, the integrated behaviour will appear familiar to those who study the gas exchange of leaves. If one wished to use the present model to estimate rates of CO₂ assimilation by leaves, one would like to assign, a priori, the values of as many parameters as possible. However, there are two key parameters which, although often correlated in vivo, show important genotypic and phenotypic variation. These are the RuP₂ carboxylase capacity of the leaf ($V_{c_{max}} = \rho k_c E_i$) and the electron transport capacity ($J_{max} = \rho j_{max}$). The way in which these two capacities vary, absolutely, and in ratio may well be a key to our understanding of the ecophysiology of plants.

We wish to thank Drs. M.R. Badger, D.T. Canvin, I.R. Cowan, H. Fock, A.E. Hall, C.B. Osmond and F.R. Whatley for useful discussions.

Symbols, units, normal values (temperature dependent parameters as at 25°C)

A ($\mu\text{mol m}^{-2} \text{s}^{-1}$)	rate of assimilation of CO ₂ (18.8*)
C (μbar)	intercellular partial pressure of CO ₂ (230*)
E (J mol^{-1})	activation energy. $Q_{10}(25^\circ\text{C}) = \exp(13.6 \cdot 10^{-6} E)$ in parentheses. k_c 58,520 (2.21), k_o 58,520 (2.21), K_c 59,356 (2.24), K_o 35,948 (1.63), m 58,520 (2.21), R_d 66,405 (2.46), $V_{c_{max}}$ 58,520 (2.21). E in Eq. (36) is 37,000 (1.65)
E_t ($\mu\text{mol g Chl}^{-1}$)	total concentration of enzyme sites (87, corresponds to 6 g carboxylase/g chl)
f	fraction of light not absorbed by chloroplasts (0.23)
ϕ (mol/mol)	ratio of oxygenation to carboxylation, Eq. (4) (0.27*)
Γ_* (μbar)	CO ₂ compensation point, without dark respiration (31*)
Γ (μbar)	CO ₂ compensation point (40*)
H (J mol^{-1})	Eq. (36) (220,000)
I ($\mu\text{mol photons m}^{-2} \text{s}^{-1}$)	irradiance (1,000*)

j ($\mu\text{Eq g Chl}^{-1} \text{s}^{-1}$)	potential rate of electron transport
J ($\mu\text{Eq m}^{-2} \text{s}^{-1}$)	as j , but on area basis
j' ($\mu\text{Eq g Chl}^{-1} \text{s}^{-1}$)	electron transport limit on rate of carboxylation, given that ϕ oxygenations occur per carboxylation
J' ($\mu\text{Eq m}^{-2} \text{s}^{-1}$)	as j' , but on area basis
j_{max} ($\mu\text{Eq g Chl}^{-1} \text{s}^{-1}$)	light saturated potential rate of electron transport (467 at 25 C)
J_{max} ($\mu\text{Eq m}^{-2} \text{s}^{-1}$)	as j_{max} , but on area basis (210 at 25 C)
k_c (s^{-1})	turnover number of RuP ₂ carboxylase (2.5)
k_o (s^{-1})	turnover number of RuP ₂ oxygenase (0.21 · k_c)
k'_c (s^{-1})	see Eq. (13) (0.585*)
K_c (μbar)	Michaelis constant for CO ₂ (460)
K_o (mbar)	Michaelis constant for O ₂ (330)
K'_c	effective Michaelis constant for free RuP ₂
m ($\mu\text{mol g Chl}^{-1} \text{s}^{-1}$)	maximum rate of reduction of PGA (436 at 25 C = 2 $k_c E_t$)
m' ($\mu\text{mol g Chl}^{-1} \text{s}^{-1}$)	PGA reduction limit on rate of carboxylation given that ϕ oxygenations occur per carboxylation
N_t ($\mu\text{mol g Chl}^{-1}$)	total concentration of NADPH and NADP ⁺ (not needed in final equations)
O (mbar)	partial pressure of O ₂ (210*)
p ($\mu\text{mol g Chl}^{-1} \text{s}^{-1}$)	limitation on rate of carboxylation given that ϕ oxygenations occur per carboxylation, of the pool size of potential acceptors, R_p
R ($\text{J K}^{-1} \text{mol}^{-1}$)	gas constant (8.314)
R	concentration of free (unbound) RuP ₂
R_t ($\mu\text{mol g Chl}^{-1}$)	concentration of free plus bound RuP ₂
R_p ($\mu\text{mol g Chl}^{-1}$)	pool size of potential acceptors, equals half the total pool of phosphate in PGA and RuP ₂ (300)
R_d ($\mu\text{mol m}^{-2} \text{s}^{-1}$)	"dark respiration" rate (1.1*)
ρ (g m^{-2})	superficial density of chlorophyll (0.45)
S ($\text{J K}^{-1} \text{mol}^{-1}$)	Eq. (36) (710)
v_c ($\mu\text{mol g Chl}^{-1} \text{s}^{-1}$)	carboxylation velocity
V_c ($\mu\text{mol m}^{-2} \text{s}^{-1}$)	as v_c , but on area basis
$V_{c\text{max}}$ ($\mu\text{mol m}^{-2} \text{s}^{-1}$)	maximum carboxylation velocity (98)
v_o ($\mu\text{mol m}^{-2} \text{s}^{-1}$)	oxygenation velocity
V'_o ($\mu\text{mol m}^{-2} \text{s}^{-1}$)	as v_o , but on area basis
$V_{o\text{max}}$ ($\mu\text{mol m}^{-2} \text{s}^{-1}$)	maximum oxygenation velocity (0.21 $V_{c\text{max}}$)
W_c ($\mu\text{mol m}^{-2} \text{s}^{-1}$)	RuP ₂ saturated rate of carboxylation
Z ($\mu\text{Eq m}^{-2} \text{s}^{-1}$)	Eq. (A2) (20)

* At standard conditions ($C=230$ [except for F], $0=210$, $I=1,000$, $T=25$ C)

Appendix 1

On the Irradiance Dependence of Potential Electron Transport. Equation (8) can only hold when $J < J_{\text{max}}$. To incorporate this upper bound we could write

$$[J - 0.5(1-f)I][J - J_{\text{max}}] = J^2 - [0.5(1-f)I + J_{\text{max}}]J + 0.5(1-f)IJ_{\text{max}} = 0 \quad (\text{A1})$$

which has the shape denoted by $Z=0$ in Fig. 11. To make the transition smoother we use the following hyperbolic equation

$$J^2 - [0.5(1-f)I + J_{\text{max}} + Z]J + 0.5(1-f)IJ_{\text{max}} = 0 \quad (\text{A2})$$

which is solved by taking the smaller root. The presence of Z adds curvature to the hyperbola as also shown in Fig. 11.

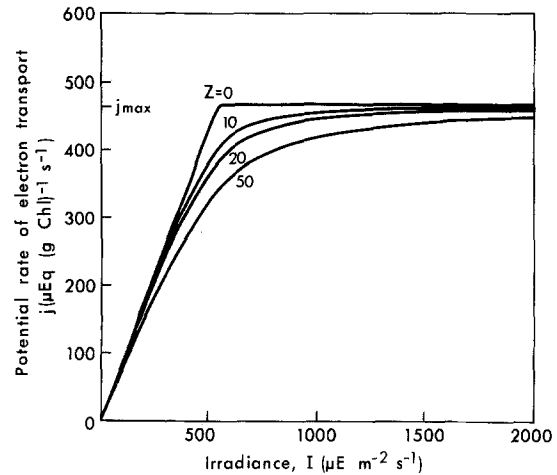


Fig. 11. Potential electron transport rate, j , versus irradiance, as calculated from Eq. (A2) in Appendix 1, after converting from an area basis J ($\mu\text{Eq m}^{-2} \text{s}^{-1}$) to a chlorophyll basis, j , by dividing by the superficial chlorophyll content, ρ ($=0.45 \text{ g Chl m}^{-2}$). The maximum potential rate, j_{max} , depends on temperature which is 25 C here; it is reached less abruptly as the parameter Z increases

Appendix 2

On the Relationship between Carboxylase Rate and RuP₂ Concentration. Equations (2) and (3) in the text were derived by Farquhar (1979), who recognised that at the high concentrations of enzyme sites found in the chloroplast stroma, only a small portion of the RuP₂ will be free, the majority being complexed to the enzyme. It is the total pool, of concentration R_t , of free and bound RuP₂, to which the regeneration of RuP₂ in the Calvin cycle directly contributes. Farquhar (1979) derived the following equation to describe the carboxylase rate, v_c

$$\left(\frac{v_c}{w_c}\right)^2 - \left(\frac{v_c}{w_c}\right) \left(1 + \frac{R_t + K'_r}{E_t}\right) + \frac{R_t}{E_t} = 0 \quad (\text{A3})$$

where w_c is the RuP₂ saturated rate given by Eq. (9). A similar quadratic equation may be written for the oxygenase in terms of w_o , its RuP₂ saturated rate. This and Eq. (A3) may be solved as

$$\frac{v_o}{w_o} = \frac{v_c}{w_c} = \frac{1}{2E_t} \{E_t + K'_r + R_t - [(E_t + K'_r + R_t)^2 - 4R_t E_t]^{\frac{1}{2}}\}$$

which is plotted as the dotted line in Fig. 3. The effective Michaelis constant, K'_r , for free RuP₂ is of the order of 20 μM (Badger and Collatz 1977) and since the stromal volume is about 25 ml/gChl (Jensen and Bahr 1977) a value for K'_r of 0.5 $\mu\text{mol/g Chl}$ was assumed for the calculation. It is apparent from Fig. 3 that the solution approximates two straight lines.

$$\text{When } R_t < E_t \frac{v_o}{w_o} = \frac{v_c}{w_c} = \frac{R_t}{E_t} \quad (\text{A5})$$

$$\text{When } R_t > E_t \quad \frac{v_o}{w_o} = \frac{v_c}{w_c} = 1. \quad (\text{A6})$$

This is so because E_t is 200 times greater than K'_v . With K'_v/E_t put to zero Eq. (A3) may be rewritten as

$$\left(\frac{v_c}{w_c} - \frac{R_t}{E_t}\right) \left(\frac{v_c}{w_c} - 1\right) = 0$$

which yields (A5) and (A6). The curvature provided by K'_v is analogous to that provided by Z in Eq. (A2).

The maximum velocities of the carboxylase and oxygenase may be written in terms of their catalytic constants, or turnover numbers, k_c and k_o , as $k_c E_t$ and $k_o E_t$, respectively. Thus Eq. (A6) may be rewritten for the carboxylase as

$$\text{For } R_t > E_t \quad v_c = \frac{k_c E_t C}{C + K_c(1 + O/K_o)} = k'_c E_t$$

and (A5) as

$$\text{For } R_t < E_t \quad v_c = \frac{R_t}{E_t} \cdot \frac{k_c E_t C}{C + K_c(1 + O/K_o)} = k'_c R_t$$

In all of the preceding, it has been assumed that the enzyme is fully activated. If the enzyme were not fully activated the turnover numbers, k_c and k_o , would need modification (Farquhar 1979).

References

- Armand, P.A., Schreiber, U., Björkman, O. (1978) Photosynthetic acclimatization in the desert shrub *Larrea divaricata*. II. Light harvesting efficiency and electron transport. *Plant Physiol.* **61**, 411-415
- Badger, M.R., Andrews, T.J. (1974) Effects of CO₂, O₂ and temperature on a high-affinity form of ribulose diphosphate carboxylase-oxygenase from spinach. *Biochem. Biophys. Res. Commun.* **60**, 204-210
- Badgar, M.R., Collatz, G.J. (1977) Studies on the kinetic mechanism of ribulose-1,5-bisphosphate carboxylase and oxygenase reactions, with particular reference to the effect of temperature on kinetic parameters. *Carnegie Inst Wash. Year Book* **76**, 355-61
- Berry, J., Farquhar, G. (1978) The CO₂ concentrating function of C₄ photosynthesis. A biochemical model. In: Proc. of the 4th International Congress on Photosynthesis, Reading, England, 1977, pp. 119-131, Hall, D., Coombs, J., Goodwin, T., eds. London. The Biochemical Soc.
- Björkman, O., Boardman, N.K., Anderson, J.M., Thorne, S.W., Goodchild, D.J., Pyliotis, N.A. (1972) Effect of light intensity during growth of *Atriplex patula* on the capacity of photosynthetic reactions, chloroplast components and structure. *Carnegie Inst. Wash. Year Book* **71**, 115-135
- Charles-Edwards, D.A. (1979) Photosynthesis and crop growth. In: Photosynthesis and plant development, pp. 111-124, Marcelle, R., ed. The Hague, Junk
- Collatz, G.J. (1978) The interaction between photosynthesis and ribulose-P₂ concentration-effects of light, CO₂ and O₂. *Carnegie Inst. Wash. Year Book* **77**, 248-251
- Ehleringer, J., Björkman, O. (1977) Quantum yields for CO₂

- uptake in C₃ and C₄ plants. Dependence on temperature, CO₂ and O₂ concentrations. *Plant Physiol.* **59**, 86-90
- Farquhar, G.D. (1979) Models describing the kinetics of ribulose biphosphate carboxylase-oxygenase. *Arch. Biochem. Biophys.* **193**, 456-468
- Graham, D. (in press) Effects of light on "dark" respiration. In: *Biochemistry of plants. A comprehensive treatise, II, General metabolism and respiration.* Davies, D.D., ed.
- Hall, A.E., Björkman, O. (1975) Model of leaf photosynthesis and respiration. In: *Ecological studies 12.* Gates, D.M., Schmerl, R.B., eds. Springer, Berlin Heidelberg New York
- Heber, U. (1976) Energy coupling in chloroplasts. *J. Bioenerg. Biomembr.* **8**, 157-172
- Heldt, H.W. (1976) Metabolite carriers of chloroplasts. In: *Transport in plants III. Intracellular interactions and transport processes*, pp. 137-143. Stocking, C.R., Heber, C., eds. Springer, Berlin Heidelberg New York
- Jensen, R.G., Bahr, J.T. (1977) Ribulose-1,5-bisphosphate carboxylase oxygenase. *Annu. Rev. Plant Physiol.* **377**-400
- Keys, A.J., Bird, I.F., Cornelius, M.J., Lea, P.J., Wallsgrave, R.M., Milfin, B.J. (1978) Photorespiratory nitrogen cycle. *Nature (London)* **275**, 741-43
- Ku, S.-B., Edwards, G.E. (1977) Oxygen inhibition of photosynthesis. I. Temperature dependence and relation to O₂/CO₂ solubility ratio. *Plant Physiol.* **59**, 986-990
- Laing, W.A., Ogren, W.L., Hageman, R.H. (1974) Regulation of soybean net photosynthetic CO₂ fixation by the interaction of CO₂, O₂ and ribulose-1,5-diphosphate carboxylase. *Plant Physiol.* **55**, 678-685
- Lilley, R. McC., Walker, D.A. (1975) Carbon dioxide assimilation by leaves, isolated chloroplasts and ribulose bisphosphate carboxylase from spinach. *Plant Physiol.* **55**, 1087-1092
- Nobel, P.S., Zaragoza, L.J., Smith, W.K. (1975) Relation between mesophyll surface area, photosynthetic rate, and illumination level during development for leaves of *Plectranthus parviflorus* Henckel. *Plant Physiol.* **55**, 1067-1070
- Nolan, W.G., Smillie, R.M. (1976) Multi temperature effects on Hill reaction activity of barley chloroplasts. *Biochim. Biophys. Acta* **440**, 461-475
- Peisker, M. (1974) A model describing the influence of oxygen on photosynthetic carboxylation. *Photosynthetica* **8**, 47-50
- Peisker, M. (1976) Ein Modell der Sauerstoffabhängigkeit des Photosynthetischen CO₂-Gaswechsels von C₃-Pflanzen. *Kulturpflanzen* **24**, 221-235
- Peisker, M., Apel, P. (1977) Influence of oxygen on photosynthesis and photorespiration in leaves of *Triticum aestivum* L. 3. Response of CO₂ gas exchange to oxygen at various temperatures. *Photosynthetica* **11**, 29-37
- Sharpe, P.S.H., De Michelle, D.W. (1977) Reaction kinetics of poikilothermic development. *J. Theor. Biol.* **64**, 649-70
- Singh, M., Ogren, W.L., Widholm, J.M. (1974) Photosynthetic characteristics of several C₃ and C₄ plant species grown under different light intensities. *Crop Sci.* **14**, 563-566
- Tenhunen, J.D., Weber, J.A., Yocum, C.S., Gates, D.M. (1979) Solubility of gases and the temperature dependency of whole leaf affinities for carbon dioxide and oxygen. *Plant Physiol.* **63**, 916-923
- West, K.R., Wiskich, J.T. (1968) Photosynthetic control by isolated pea chloroplasts. *Biochem J.* **109**, 527-32
- Wong, S.C. (1979) Stomatal behaviour in relation to photosynthesis. Ph. D. Thesis A.N.U.
- Woo, K.C., Berry, J.A., Turner, G.L. (1978) Release and refixation of ammonia during photorespiration. *Carnegie Inst. Wash. Year Book* **77**, 240-245

Received 12 July, 1979; accepted 9 December 1979